Structural basis of activation-dependent binding of ligand-mimetic antibody AL-57 to integrin LFA-1

Hongmin Zhang[a,1], Jin-huan Liu[a], Wei Yang[b,c,2], Timothy Springer[b,c,3], Motomu Shimaoka[b,d], and Jia-huai Wang[a,3]

[a]Dana-Farber Cancer Institute, Department of Pediatrics, and Department of Biological Chemistry and Molecular Pharmacology, and Departments of [c]Pathology and [d]Anesthesia, Harvard Medical School, Boston, MA 02115; and [b]Immune Disease Institute and Program in Cellular and Molecular Medicine, Children's Hospital Boston, Boston, MA 02115

Contributed by Timothy Springer, August 21, 2009 (sent for review June 15, 2009)

The activity of integrin LFA-1 ($\alpha_L\beta_2$) to its ligand ICAM-1 is regulated through the conformational changes of its ligand-binding domain, the I domain of α_L chain, from an inactive, low-affinity closed form (LA), to an intermediate-affinity form (IA), and then finally, to a high-affinity open form (HA). A ligand-mimetic human monoclonal antibody AL-57 (activated LFA-1 clone 57) was identified by phage display to specifically recognize the affinity-upregulated I domain. Here, we describe the crystal structures of the Fab fragment of AL-57 in complex with IA, as well as in its unligated form. We discuss the structural features conferring AL-57's strong selectivity for the high affinity, open conformation of the I domain. The AL-57-binding site overlaps the ICAM-1 binding site on the I domain. Furthermore, an antibody Asp mimics an ICAM Glu by forming a coordination to the metal-ion dependent adhesion site (MIDAS). The structure also reveals better shape complementarity and a more hydrophobic interacting interface in AL-57 binding than in ICAM-1 binding. The results explain AL-57's antagonistic mimicry of LFA-1's natural ligands, the ICAM molecules.

cell adhesion | crystal structure | ICAM-1

Integrins are major cell adhesion molecules, mediating cell-cell and cell-extracellular matrix interactions. Integrin molecules consist of noncovalently associated α and β transmembrane polypeptide chains. Lymphocyte function-associated antigen-1 (LFA-1, $\alpha_L\beta_2$ or CD11a/CD18) represents the predominant integrin on lymphocytes. By binding to its major Ig superfamily (IgSF) ligand ICAM-1 (intercellular adhesion molecule-1), and to other ICAM family members, LFA-1 plays a vital role in adhesive interactions with both vascular endothelial cells and antigen-presenting cells (1–3). Integrin's activity is dynamically regulated by bidirectional transmembrane signaling. In lymphocytes, the ability of LFA-1 to bind ICAM-1 is rapidly upregulated in response to the intracellular signaling elicited by activation of other receptors, including chemokine and T cell receptors (inside-out signaling). Conversely, the binding of ICAM-1 to LFA-1 transmits signals to the cytoplasm, thereby altering gene expression and cellular metabolism (outside-in signaling) (4, 5).

The ligand-binding domain of LFA-1, which has been designated an inserted (I) domain of approximately 200 amino acids (aa) in the α_L subunit, forms an independent Rossmann fold with a central β sheet flanked by seven α helices. A divalent ion is located at the upper side of the domain in a metal ion-dependent adhesion site (MIDAS) (6), to which ICAM-1 binds. The C-terminal part of the I domain comprising the α7 helix and the preceding β6-α7 loop is conformationally mobile, adopting three distinct conformations: closed, intermediate, and open. The wild-type, ICAM-1-unbound I domain possesses both the low-affinity configuration of the MIDAS and the closed conformation of the C-terminal part. ICAM-1 binding to the MIDAS stabilizes its high-affinity configuration. This change at the MIDAS is linked to the downward shift of the I domain's α7 helix one to two helical turns and to the reshaping of the β6-α7 loop, progressively inducing the intermediate and open conformations, respectively. The downward shift of the α7 helix would typically relay the outside-in conformational signals within the LFA-1 ecto-domain toward the cytoplasm. Conversely, inside-out signals facilitate the induction of the downward shift of the I domain α7 helix, which is allosterically linked to the conversion of the MIDAS to the high-affinity configuration (5). In this way, those conformational changes of the I domain involving an allosteric coupling of the MIDAS configuration and the conformation of the C-terminal part constitute an essential mechanism for transmitting bidirectional signals and integrin affinity regulation (7). From energetic point of view, signaling molecules have population distribution among different conformational states on evolutionarily selected energy landscape. Stimulants from inside or outside cell will remodel this landscape and shift the population distribution, biasing toward a particular downstream functional event (8).

Most antibodies against integrin I domains bind equally well to the alternative conformations. However, two known antibodies are activation-dependent and bind significantly better to the higher affinity conformation of the I domain. Mouse anti-human Mac-1 monoclonal antibody (mAb) CBRM1/5 binds only the active integrin Mac-1 (9). The epitope was mapped to the β1-α1 loop, the α3 helix, and α3-α4 loop in the activated form of the I domain (10). More recently, AL-57 (activated LFA-1 clone 57), was selected by a phage display that targeted a mutationally stabilized HA domain, versus the default, wild-type LA LFA-1 I domain (11). AL-57 functions as an ICAM-1 mimetic antibody that exhibits several key features of the ICAM-1/LFA-1 interaction. Not only do AL-57 and ICAM-1 both bind progressively better as LFA-1 affinity increases, they both require Mg^{2+} for binding. However, certain underlying structural features remain unclear; e.g., how does AL-57 preferentially recognize the higher affinity I domain, and does AL-57 binding to the I domain compel a conversion to the open the conformation? Here, we describe crystal structures of the Fab fragment of the AL-57 in complex with LFA-1 I domain and of the Fab alone. The comparative studies we carried out reveal AL-57 as the only known ligand-mimetic mAb to LFA-1. The structures also explain AL-57's binding preference for the high affinity I domain conformation and how it competes against ICAM-1 binding.

Results and Discussion

The Overview. To understand the molecular mechanism of AL-57's activation-dependent binding and to see whether, like

Author contributions: T.S., M.S., and J.-h.W. designed research; H.Z., J.-h.L., M.S. and J.-h.W. performed research; W.Y. contributed new reagents/analytic tools; T.S. and M.S. analyzed data; and H.Z., T.S., M.S., and J.-h.W. wrote the paper.

The authors declare no conflict of interest.

Data deposition: The atomic coordinates have been deposited in the Protein Data Bank, www.pdb.org (PDB ID codes 3HI5 and 3HI6).

[1]Present address: Department of Physiology, the University of Hong Kong, Hong Kong, China.

[2]Present address: Beijing Novo Nordisk Pharmaceuticals Science and Technology Co. Ltd, No. 29 Life Science Park Road, Changping District, Beijing, 102206, People's Republic of China.

[3]To whom correspondence may be addressed. E-mail: jwang@red.dfci.harvard.edu or springer@idi.harvard.edu.

Table 1. Data reduction and refinement statistics

	AL-57	AL-57/IA
Space group	$P6_122$	$P6_5$
a, Å	84.7	133.8
b, Å	84.7	133.8
c, Å	317.2	161.1
α, °	90	90
β, °	90	90
γ, °	120	120
Molecule/asymmetric unit	1	2
Wavelength, Å	0.97924	0.97937
Resolution, Å	20–2.50	30–2.30
Unique reflections	19,789	67,977
Completeness, %	92.4 (60.2)	97.8 (78.8)
R_{sym}, %	7.5 (36.1)	8.4 (47.4)
$I/\sigma(I)$	29.1 (3.0)	23.8 (2.3)
Redundancy	12.6 (6.3)	7.4 (4.9)
Total no. of reflections		
Work	18,783	64,528
Test	1,006	3,449
R/R_{free}, %	23.42/27.68	17.04/22.57
Ramachandran plot		
Favored, %	95.8	97.2
Allowed, %	99.5	100
Outlier, %	0.5	0.0
No. of atoms		
Protein	3,280	9,398
Water	54	700
Average *B* factor, Å^2	39.3	23.1
rmsd from ideal values		
Bond lengths, Å	0.009	0.009
Bond angles, °	1.152	1.142

Numbers in parentheses are for the highest resolution shell. $R_{sym} = \Sigma_{hkl}|I-\langle I\rangle|/\Sigma I$, where I is the observed intensity and $\langle I\rangle$ is the average intensity from observations of symmetry-related reflections. A subset of the data (5%) was excluded from the refinement and used to calculate R_{free}. $R = \Sigma||F_o|-|F_c||/\Sigma|F_o|$.

ICAM-1, the binding of AL-57 to the I domain forces its conversion to the higher-affinity I domain, we decided to co-crystallize AL-57 with the disulfide-stabilized IA I domain mutant (L161C/F299C). In the absence of bound ICAM-1, the IA I domain mutant (L161C/F299C) assumes the low-affinity MIDAS conformation, with the C-terminal α7 helix and β6-α7 loop of the domain mutationally stabilized in the intermediate conformation (7). However, in the complex structure of ICAM-1/IA, the MIDAS is converted to a high-affinity conformation and the C-terminal portion changes into an open conformation (7). We wanted to see at an atomic level whether AL-57, as a ligand-mimetic, would favor these conformational changes as well.

Cocrystals in the space group $P6_5$ diffracted to 2.3 Å. The structure was determined using molecular replacement, locating two complexes in one asymmetric unit. There are no significant structural variations between the two independent AL-57/IA complexes. AL-57 Fab alone was crystallized in a distinct condition. The crystals are in space group $P6_122$ with one molecule per asymmetric unit and diffracted to 2.5 Å. The structure was similarly solved using molecular replacement. Table 1 gives the crystallographic data and the refinement statistics.

Fig. 1 depicts two views of the Cα trace of the AL-57/IA complex A (in green) with unligated AL-57 Fab (in orange) and an unligated intermediate affinity LFA-1 I domain (in pink) superimposed on the corresponding domains for comparison. In this figure, the AL-57 superposition is based upon the variable domains of the antibody, the Fv module. The constant module

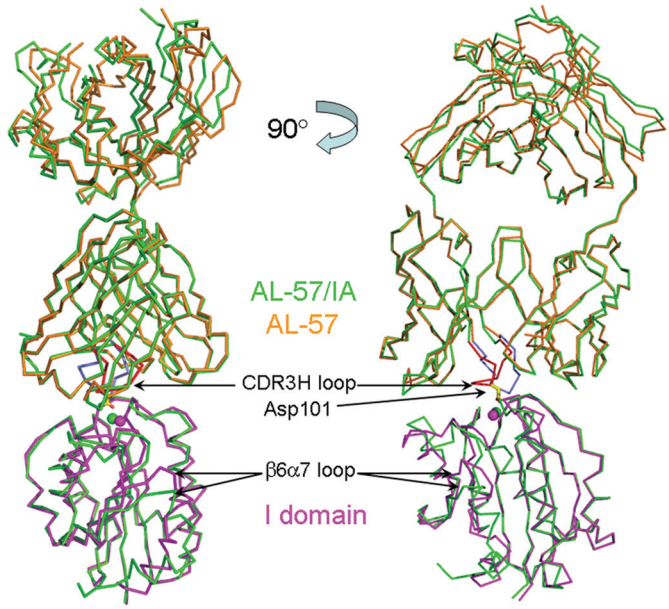

Fig. 1. Two views of the AL-57 and AL-57/IA structures. The AL-57 and AL-57/IA structures are shown as Cα traces with AL-57 colored in orange and AL57/IA in green. The AL-57 was superimposed onto AL-57/IA based on the variable region of AL-57. There is roughly an 8° rotation for the constant domain of unligated AL-57 compared to ligated AL-57. An unligated intermediate affinity LFA-1 I domain (PDB code 1MJN) colored in pink was superimposed onto the IA in the AL-57/IA structure. Asp-101 from the CDR3H loop of AL-57/IA is colored with yellow carbons and shown in a stick model. The CDR3H loop of AL-57/IA was colored in red and the CDR3H loop of AL-57 alone was colored in purple. Asp-101 coordinated to a metal ion (shown as a green sphere) in the MIDAS of IA. The metal ion in unligated I domain (1MJN) was shown as a pink sphere.

C_L/C_{H1} showed a rigid-body approximately 8° rotation compared to the orientation in unbound AL-57. The most interesting change stemming from ligation was associated with the CDR3H loop of the heavy chain's variable domain V_H. In the unligated AL-57 structure, the electron density for this loop was the poorest of all. The entire loop was less well ordered. The main chain of CDR3H loop can still be traced without ambiguity, and the loop appears to extend straight away from AL-57 (colored in purple in Fig. 1). However the side chains for the key integrin-binding residue Asp-101(H) and its neighboring Phe-102(H) were very mobile and difficult to define. Upon binding to IA, Asp-101(H) coordinated the metal ion on MIDAS, which brought the complete CDR3H loop into order and changed its conformation to bend toward the body of AL-57 (colored in red in Fig. 1).

With Asp-101(H) coordination, the MIDAS of the IA domain changed from a closed conformation into an open one. Fig. 2 depicts the metal ion's coordination at the MIDAS region of three structures. The MIDAS is in open conformation in both Fig. 2*A* (from AL-57/IA) and Fig. 2*B* (from ICAM-3/HA; PDB code 1T0P), but is in closed conformation in Fig. 2*C* (from unligated intermediate affinity LFA-1 I domain; PDB code 1MJN). It is clear that the IA domain underwent structural alterations upon AL-57 binding, similar to what was observed when IA domain was bound to ICAM-1, as described in detail below.

AL-57 Preferentially Binds to the Affinity-Upregulated I Domain. The characteristic feature of LFA-1's authentic ligands, namely ICAM-1 and the other ICAM family members, is that they preferentially bind to the affinity-upregulated I domain (12).

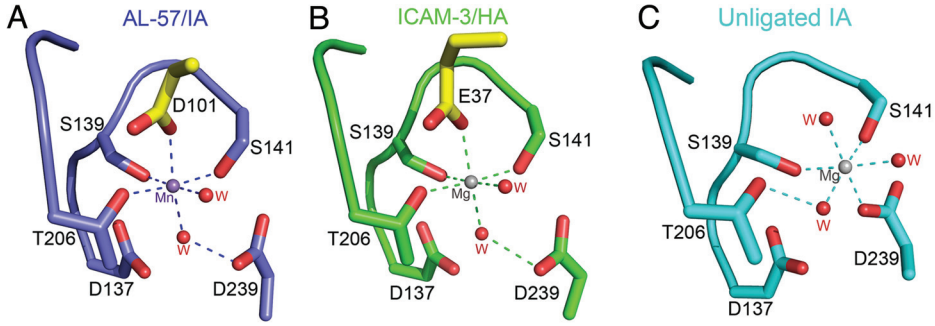

Fig. 2. MIDAS of the I domain in different conformations. The MIDAS residues of the I domain are shown as stick models and colored with purple carbon atoms in IA in the AL-57/IA structure (*A*), green carbon atoms in HA in the ICAM-3/HA structure (*B*, PDB code 1T0P) and cyan carbon atoms in the unligated IA with closed conformation (*C*, PDB code 1MJN). Acidic residues from ligands D101 in AL-57 (*A*) and E37 in ICAM-3 (*B*), are also shown as stick models with yellow carbon atoms. All oxygen atoms are in red. Metal ions in the MIDAS are labeled and shown as spheres. Waters in MIDAS are shown as red spheres and labeled with a ''w.'' Coordination bonds are shown as dashed lines. Compared to the closed conformation in the unligated IA, in which D239 coordinated to the MIDAS metal ion directly (*C*), D239 in IA(*A*) or HA (*B*) coordinated to the metal ion via a water molecule and the metal ion shifted about 2.3Å and coordinated to T206 directly.

This is a tendency also shared by the AL-57 antibody. Both a cell-binding assay (13) and surface plasmon resonance (SPR) analysis (11) showed that the monoclonal antibody AL-57 discriminates among wild-type low-affinity LA, mutationally-stabilized intermediate-affinity IA, and mutatationally-stabilized high-affinity HA states of LFA-1. With SPR, AL-57 showed no binding to LA domain, but binding to IA and HA domains with K_D being approximately 4.7 μM and 0.023 μM, respectively (11). The binding preference of AL-57 has now been demonstrated by comparative structural studies. Early structural data have shown that ICAM family members share the same binding mode to the LFA-1 I domain (7, 14, 15). Central in the binding site is an invariant acidic residue designated Glu-37 (the residue numbering follows ICAM-3's nomenclature throughout) coordinating to the MIDAS metal ion. With the wild-type or unligated intermediate affinity IA I domain, the MIDAS was in a closed conformation (Fig. 2*C*), wherein one acidic MIDAS residue (Asp-239) directly coordinated the metal, along with Ser-139 and Ser-141 on the β1-α1 loop. Another MIDAS residue (Thr-206) bound to the metal indirectly via a water molecule. There was one additional water molecule that completed the coordination geometry. By contrast, ligation stabilized the geometry of MIDAS in an open conformation (Fig. 2*B*, from ICAM-3/HA structure). In the open conformation, the acidic residue Asp-239 moved away into the secondary coordination sphere. Since an acidic I domain residue no longer directly coordinates the metal, this altered metal coordination most likely strengthens the interaction between the metal ion and the acidic residue from the ligand. In this case, it is the ligand that donates the only negatively charged oxygen to the primary coordination sphere. Again, there was one additional water molecule completing the coordination geometry. Ligand-binding was also accompanied by a 2.3 Å ''sideways'' movement of the metal ion (5). Interestingly, upon AL-57 binding to the I domain, the acidic residue Asp-101 from AL-57's CDR3H loop played the same role as Glu-37 of ICAM did. In the AL-57/IA structure (Fig. 2*A*), this Asp-101(H) completes the octahedral coordination geometry of the metal in IA's MIDAS. Thus, the direct coordination of an acidic residue to the MIDAS of the I domain in an open conformation is a key structural feature shared by the authentic ligand and AL-57. Furthermore, other coordinating MIDAS residues also slightly shift in the same direction for AL-57/IA and ICAM-1/IA structures, compared to those MIDAS residues in the closed conformation.

Another hallmark structural alteration from the closed to the open conformation of the I domain upon AL-57 or ICAM binding is that a conserved Gly-240 in the β4-α5 loop of I domain flips its main chain conformation such that the β4-α5 loop bends away from the binding surface. This flipping of Gly-240 is coupled to the movement of the immediately neighboring Asp-239, which pulls this MIDAS coordinating residue away from any direct coordination to the metal, as discussed above. Consequently, the flipping movement also leads to the reorientation of the downstream neighboring Glu-241 into a favorable position, enabling a crucial electrostatic interaction to the basic residue Lys-42 from ligand ICAM-3 (or Lys-39 in ICAM-1 and Arg-42 in ICAM-5) (7, 14, 15). In the current AL-57/IA structure, there occurred a similar interaction between Glu-241 and AL-57's Arg-31(H) (Fig. 3*A*). It is noteworthy that this main chain flipping can only occur when a Gly occupies the I domain's position 240 as a conserved residue (3). Apparently, the concerted movement of Asp-239-Gly-240-Glu-241, located on the β4-α5 loop, one of the MIDAS loops, is characteristic of allosteric conformational changes to the I domain upon ligand-binding. Thus, the AL-57/IA structure revealed two key features, which AL-57 shares with ICAMs, supporting preferential binding to the affinity-upregulated I domain: Asp-101 on CDR3H, which directly coordinates to the open MIDAS configuration; and Arg-31 on CDR1H, which forms an electrostatic interaction with Glu-241 in the open conformation.

In contrast to the above discussion on Asp-101(H) and Arg-31(H), residue Trp-103 in the flexible CDR3H loop of AL-57 plays a unique role in favoring binding to the affinity-upregulated I domain, which is observed only in AL-57 and not in ICAM. Trp-103(H) formed a hydrogen bond from its indole ring to the carboxyl group of Asp-239 on the α_L β4-α5 loop (Fig. 4). In turn, this MIDAS residue Asp-239 indirectly bound to the metal via a water molecule (Fig. 2*A* and Fig. 4). In this way, binding to ligand orients the side chain of Trp-103(H) in AL-57. Compared with the wild-type closed conformation LA I domain, both the β5-α6 and β6-α7 loops of the open conformation moved downward in the direction indicated by the arrows in Fig. 4. Consequently, His-264 on the β5-α6 loop had its imidazole ring snugly sandwiched between Trp-103(H) and Trp-52(H) of AL-57. By contrast, the wild-type LA was in a closed conformation with the β5-α6 loop closer to the MIDAS. Should the AL-57 antibody have approached LA domain, the side chain of His-264 would have collided with the Trp-103(H) (See Fig. 4, a magenta-colored His-264's sidechain clashes with Trp-103 of AL-57). This may explain why AL-57/LA binding is not detectable, further demonstrating AL-57's binding preference.

This begs the question: why does AL-57 bind in a stronger fashion to HA than to IA I domain? As mentioned before, AL-57 binding triggers IA domain to change its conformation to an open state, similar to HA, and to what was observed when ICAM-1 bound to IA domain (7). ICAM-1 binding to the

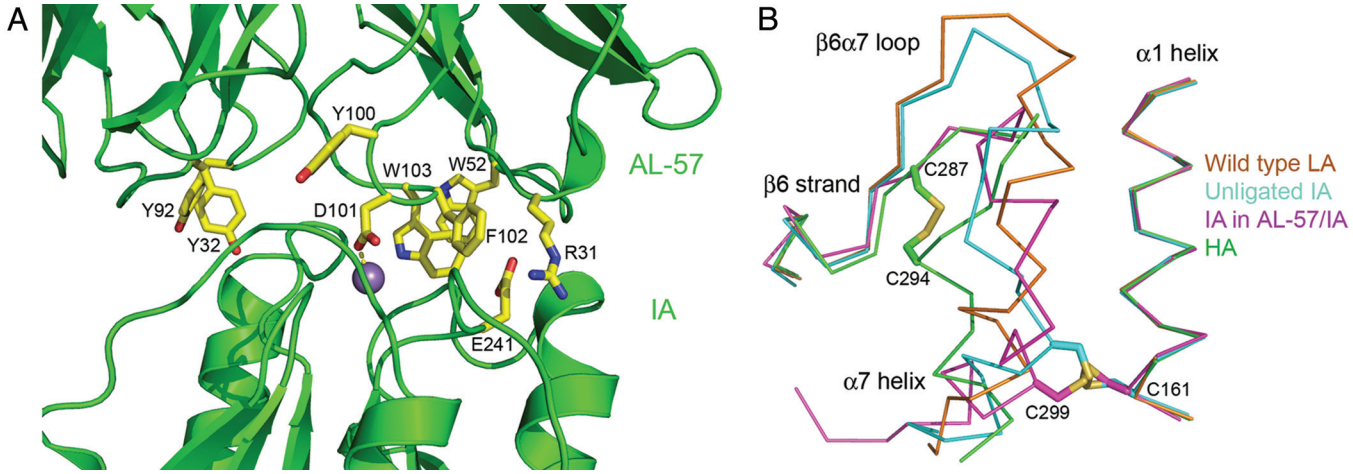

Fig. 3. (*A*) Interacting residues in the binding interface. Aromatic residues from AL-57, which contribute a significant level of hydrophobic interaction, are shown as stick models with yellow carbons. E241 from IA and R31(H) from AL-57, which form electrostatic interactions, are also shown as stick models with yellow carbons. The metal ion in MIDAS is shown as a purple sphere. D101(H) from AL-57 is shown as a stick model in yellow. (*B*) The movement of the C-terminal α7 helix in IA. The wild-type LA (PDB code 3F74), unligated IA (PDB code 1MJN), IA in the AL-57/IA complex, and HA in the ICAM-3/HA (PDB code 1T0P) complex, were superimposed and colored in gold, cyan, magenta, and green, respectively. For clarity, only the α1 helices, β6 strands, β6-α7 loops, and α7 helices are shown as Cα traces. The engineered disulfide bonds (Cys-161-Cys-299 in IA and Cys-287-Cys-294 in HA) are shown as stick models. Compared to unligated IA, the β6-α7 loop of IA in AL-57/IA complex moved downward like that observed in HA, indicating an open conformation.

MIDAS allosterically induced the reshaping of a remote β6-α7 loop and the downward axial displacement of the C-terminal helix, thereby relaying outside-in conformational signaling toward the cytoplasm. Fig. 3*B* depicts a local area with four structures overlaid: HA, IA, and IA in AL-57 complex along with a closed, LA I domain for comparison. The β6-α7 loop of unligated IA is in the intermediate position between the open and closed conformations. However, the β6-α7 loop of IA in the AL-57 complex is in the open conformation, just like that of HA. Because of the strain imposed by the engineered disulfide bond between Cys-161 and Cys-299, the middle portion (where Cys-299 is located) of the IA's C-terminal helix α7 has been restrained. This makes the α7 helix end at Gln-303, as opposed to Ile-306 in unligated IA. All of these factors cost energy and likely contribute to the relatively low affinity of the AL-57/IA interaction, compared to that of the AL-57/HA interaction.

The Uniqueness of AL-57 Among Antibodies to Integrin I Domains. The direct metal coordination from an acidic residue and the induced concerted movement of Asp-239-Gly-240-Glu-241 on I domain's β4-α5 loop discussed above revealed the ligand-mimetic features of AL-57 when it binds to the LFA-1 I domain. Moreover, AL-57 is not only ligand-mimetic, but also binds with higher affinity than the native ligand. SPR measurements have shown that the affinity of AL-57 binding to the high-affinity I domain of LFA-1 is about 6-fold higher than that of ICAM-1 binding. In particular, the off-rate for AL-57 binding is 0.0055 $s^{-1}\times 10^2$, as opposed to 1.4 $s^{-1}\times 10^2$ for ICAM-1 binding; in other words, more than 250-fold slower for AL-57-binding than for ICAM-1-binding (11). The buried surface area of the AL-57/IA complex is 1864 Å^2, which is slightly higher than average value of 1,680 Å compared with other antibody/antigen values (16). However, the interface's shape complementary index (Sc value) is 0.78, sig-

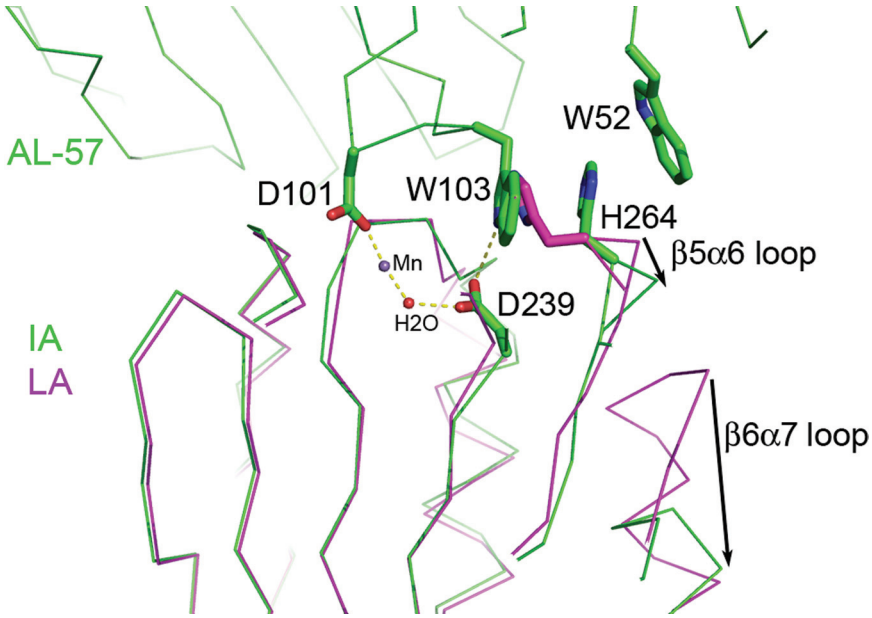

Fig. 4. Conformational changes to the I domain in AL-57/IA compared to the wild-type low-affinity I domain (LA, PDB code 1LFA). LA was superimposed onto the IA in the AL-57/IA complex. These structures are shown as Cα traces with AL-57 and IA in green and LA in pink. Three residues from AL-57 (D101, W103, and W52) and two residues (D239 and H264) from IA were colored with green carbons and shown as stick models. Residue H264 from LA was colored with magenta carbons and shown as a stick model. The metal ion and a water molecule from IA were shown as a purple and red sphere, respectively. The hydrogen bonds from D239 of IA to W103 of Fab and a water molecule, as well as the coordination bonds between the metal ion and Fab's D101 are shown in yellow dash lines. Conformational changes of IA compared to those of LA in the β5-α6 and β6-α7 loops are indicated by black arrows. H264 in IA moved away from the MIDAS compared to H264 in LA.

nificantly higher than the average antibody/antigen value of 0.66 (17), and is indicative of an excellent fit between AL-57 and IA domain in the complex. Notably, the buried surface area of ICAM-1/IA complex is only 1,250 Å^2 (7), much smaller than that of AL-57/IA. Its Sc value is 0.73, also lower than that of AL-57/IA. Furthermore, the AL-57/IA interface displays a remarkable cluster of aromatic residues from AL-57 (Fig. 3*A*). These include Trp-52 of CDR2H, Tyr-100, Phe-102, and Trp-103 of CDR3H, as well as Tyr-32 of CDR1L and Tyr-92 of CDR3L. This kind of hydrophobic cluster is not seen in the interface between ICAMs and the I domain (14, 15). The highly hydrophobic nature of the AL-57 interface clearly explains the 250-fold slower off-rate of AL-57 binding to the high-affinity α_L I domain compared to that observed in ICAM-1 binding, as demonstrated in our comparative binding studies on ICAM-1 and ICAM-3 (14). Overall, such highly favored interface and binding kinetics strongly suggest that AL-57 acts as a ligand-mimetic that is strongly competitive with the native ligand.

An earlier report systematically studied the binding sites of numerous mAbs characterized to bind the α_L I domain (18). Notably, none of these mAbs recognized species specific residues bound by ICAM-1, or were metal ion-dependent. The mAb were classed as competitive antagonists if they inhibited binding by both wild-type activated LFA-1 and HA LFA-1, and allosteric antagonists if they inhibited binding by wild-type activated LFA-1 but not HA LFA-1 (19, 20). All competitive mAb bound near the ICAM binding site, and one agonistic mAb bound distant from this site. All mAb recognizing epitopes in the first residue of the α1-helix and in the α3-α4 loop, which are adjacent in the structure and show little conformational movement, were competitive antagonists. In contrast, among mAb that bound to a group of seven adjacent residues in the β5-α6 loop and α6-helix, which show substantially more conformational movement, one mAb was a competitive antagonist and two were allosteric antagonists (18).

The mAb CBRM1/5 selectively recognizes the high affinity conformation of the α_M I domain (9). However, binding does not require metal ion. Furthermore, mapping of the CBRM1/5 epitope shows it binds to the β1-α1 loop and the α3 helix and α3-α4 loop (10). The residues in the epitope are in a conformationally mobile region on one side only of the MIDAS. These results suggest that the epitope does not include the MIDAS.

There is one structural report of mAb binding to the MIDAS of the I domain from a different integrin. This is the inhibitory monoclonal antibody AQC2, which acts against the I domain of $\alpha_1\beta_1$ integrin (21). Despite containing an acidic residue from AQC2 binding to the metal ion on MIDAS, in a fashion similar to that of a natural ligand, the I domain remains in the closed form. This is intriguing. A close examination demonstrates that the important Asp-257-G258-Glu-259 motif on the β4-α5 loop of α_1 I domain is, indeed, in a closed conformation. One key fact is that the Glu-259 of the α_1 I domain, the counterpart to Glu-241 of the α_L I domain discussed above, does not have its crucial salt bridge partner from AQC2 to thus consolidate the binding. The main chain conformation of Gly-258 does not flip so that the β4-α5 loop still keeps pointing upwards like that in the unligated I domain. There is no water molecule to bridge the interaction between the metal and Asp-257, as is commonly seen in the open conformation, which further confirms the closed conformation status of AQC2. Therefore, AQC2 is not a ligand-mimetic. It binds closed conformation of I domain, and exerts its inhibitory effect via sterically blocking ligand-binding to the α_1 I domain.

A very recent report describes a structure of LFA-1 I domain in complex with the Fab portion of humanized monoclonal IgG_1 antibody, Efalizumab, which is clinically approved drug for treating patients with psoriasis (22). In that structure, Fab binds to the side of the I domain on the α1 and α3 helices, i.e., to the same epitope as one group of previously mapped competitive antagonist mAbs (18). As the binding does not trigger any conformational changes, the I domain remains in a closed, low-affinity conformation. The most interesting aspect of this structure is that the Efalizumab epitope on the LFA-1 I domain does not overlap with the ICAM-1-binding region *per se*. Instead, the drug's inhibitory effect stems from the steric hindrance between the antibody's light chain and the ICAM-1 domain 2.

The conclusion from our AL-57/IA complex structure studies is that AL-57 represents an example of a monoclonal antibody that binds to the α_L I domain in a ligand-mimetic fashion, and which discriminatively acts upon the affinity-upregulated I domain. This contrasts with the clinically approved mAb to LFA-1, which binds to the closed conformation of I domain and sterically blocks ligand-binding. An mAb like AL-57 may have favorable pharmacokinetics with long half-life in vivo, and have fewer potential side effects (13).

The unique features of AL-57 may in part derive from the fact that it was isolated from an artificial, human-like antibody library displayed in phage (17). Thus, it has not been negatively selected against self, as are natural antibodies. Natural antibodies recognize species-specific differences. The species-specific residues in LFA-1 that are in ICAM contact regions and recognized by mAb have previously been compared (18). Although species-specific residues are present in the ICAM contact region, they appear to be scarcer than in the epitopes recognized by an extensively mapped subset of antibodies. The uniqueness of AL-57 may also in part be attributable to the strong selection against the low affinity conformation and for the high affinity conformation during its isolation. The structural studies reported here suggest that it should in principle be possible to obtain antibodies that faithfully mimic highly conformationally-specific biological interactions, for a wide range of biological and pharmaceutical applications.

Methods

Protein Production and Crystallization. The α_L IA domain was expressed in *E. coli*, refolded, and purified as previously described (7). The IA protein was concentrated and exchanged into a buffer containing 10 mM HEPES pH 7.5, 50 mM sodium chloride, and 5 mM manganese chloride. A Fab fragment of antibody AL-57 was prepared as described (11). Crystals were obtained using hanging droplet vapor diffusion. One microliter of Fab at 20 mg/mL was mixed with 1 μL of reservoir buffer in 0.1 M cacodylate pH 6.4, 0.2 M $Zn(Ac)_2$, 18% PEG8000. The cryoprotectant for crystals of Fab alone is 0.1 M cacodylate pH 6.4, 20% glycerol and 30% PEG8000. One microliter of an equal molar mixture of Fab and IA at a total concentration of 18 mg/mL was mixed with 1 μL of reservoir buffer in 0.1 M sodium acetate, pH 5.5, 2.0 M $(NH_4)_2SO_4$. The cryoprotectant for the complex crystals is 0.1 M sodium acetate, pH 5.5, 2.0 M $(NH_4)_2SO_4$, 0.3 M sodium citrate.

Structure Determination. Crystals were harvested and soaked in the cryoprotectant and then flash frozen into liquid nitrogen. The diffraction data were collected using the beamline 19ID at Argonne National Laboratory and processed with HKL2000 (23). Molecular replacement was performed to determine the structure using the program Phaser from CCP4 (24). IA domain from the complex of ICAM1-IA (PDB code 1MQ8) and the Fab fragment from PDB 1MHP (the structure of the α_1 I domain in complex with Fab) were used as the search model. The variable region of Fab (with CDR loops deleted) was used as the first search model, IA domain as the second, and the constant region of Fab as the last search model. The complex was refined with Refmac and cycled with model rebuilding using Coot (25). TLS refinement was incorporated into the later stages of the refinement process. The final model was analyzed with MolProbity (26). The coordinates of the Fab alone, and in complex with IA, have been deposited in the Protein Data Bank with the codes 3HI5 and 3HI6, respectively.

ACKNOWLEDGMENTS. This work has been supported by National Institutes of Health Grants HL48675 (to J.H.W. and M.S.), CA31798 (to T.A.S.), and AI063421 (to M.S.).

1. Grakoui A, et al. (1999) The immunological synapse: A molecular machine controlling T cell activation. *Science* 285:221–227.
2. Springer TA (1994) Traffic signals for lymphocyte recirculation and leukocyte emigration: The multistep paradigm. *Cell* 76:301–314.
3. Springer TA, Wang JH (2004) The three-dimensional structure of integrins and their ligands, and conformational regulation of cell adhesion. *Adv Protein Chem* 68:29–63.
4. Hynes RO (2002) Integrins: Bidirectional, allosteric signaling machines. *Cell* 110:673–687.
5. Luo BH, Carman CV, Springer TA (2007) Structural basis of integrin regulation and signaling. *Annu Rev Immunol* 25:619–647.
6. Lee JO, Rieu P, Arnaout MA, Liddington R (1995) Crystal structure of the A domain from the alpha subunit of integrin CR3 (CD11b/CD18). *Cell* 80:631–638.
7. Shimaoka M, et al. (2003) Structures of the alphaL I domain and its complex with ICAM-1 reveal a shape-shifting pathway for integrin regulation. *Cell* 112:99–111.
8. Smock RG, Gierasch LM (2009) Sending signals dynamically. *Science* 324:198–203.
9. Diamond MS, Springer TA (1993) A subpopulation of Mac-1 (CD11b/CD18) molecules mediates neutrophil adhesion to ICAM-1 and fibrinogen. *J Cell Biol* 120:545–556.
10. Oxvig C, Lu C, Springer TA (1999) Conformational changes in tertiary structure near the ligand binding site of an integrin I domain. *Proc Natl Acad Sci USA* 96:2215–2220.
11. Shimaoka M, et al. (2006) AL-57, A ligand-mimetic antibody to integrin LFA-1, reveals chemokine-induced affinity up-regulation in lymphocytes. *Proc Natl Acad Sci USA* 103:13991–13996.
12. Shimaoka M, et al. (2001) Reversibly locking a protein fold in an active conformation with a disulfide bond: Integrin alphaL I domains with high affinity and antagonist activity in vivo. *Proc Natl Acad Sci USA* 98:6009–6014.
13. Huang L, et al. (2006) Identification and characterization of a human monoclonal antagonistic antibody AL-57 that preferentially binds the high-affinity form of lymphocyte function-associated antigen-1. *J Leukoc Biol* 80:905–914.
14. Song G, et al. (2005) An atomic resolution view of ICAM recognition in a complex between the binding domains of ICAM-3 and integrin alphaLbeta2. *Proc Natl Acad Sci USA* 102:3366–3371.
15. Zhang H, et al. (2008) An unusual allosteric mobility of the C-terminal helix of a high-affinity alphaL integrin I domain variant bound to ICAM-5. *Mol Cell* 31:432–437.
16. Lo Conte L, Chothia C, Janin J (1999) The Atomic Structure of Protein-Protein Recognition Sites. *J Mol Biol* 285:2177–2198.
17. Lawrence MC, Colman PM (1993) Shape complementarity at protein/protein interfaces. *J Mol Biol* 234:946–950.
18. Lu C, Shimaoka M, Salas A, Springer TA (2004) The binding sites for competitive antagonistic, allosteric antagonistic, and agonistic antibodies to the I domain of integrin LFA-1. *J Immunol* 173:3972–3978.
19. Lu C, et al. (2001) An isolated, surface-expressed I domain of the integrin alphaLbeta2 is sufficient for strong adhesive function when locked in the open conformation with a disulfide bond. *Proc Natl Acad Sci USA* 98:2387–2392.
20. Yang W, Shimaoka M, Salas A, Takagi J, Springer TA (2004) Intersubunit signal transmission in integrins by a receptor-like interaction with a pull spring. *Proc Natl Acad Sci USA* 101:2906–2911.
21. Karpusas M, et al. (2003) Crystal structure of the alpha1beta1 integrin I domain in complex with an antibody Fab fragment. *J Mol Biol* 327:1031–1041.
22. Li S, et al. (2009) Efalizumab binding to the LFA-1 alphaL I domain blocks ICAM-1 binding via steric hindrance. *Proc Natl Acad Sci USA* 106:4349–4354.
23. Otwinowski Z, Minor W (1997) Processing of X-ray diffraction data collected in oscillation mode. *Macromolecular Crystallography, Methods in Enzymology*, eds Carte CW, Jr, Sweet RM (Academic, London), Vol 276, pp 307–326.
24. CCP4 (1994) The CCP4 suite: Programs for protein crystallography. *Acta Crystallogr D* 50:760–763.
25. Emsley P, Cowtan K (2004) Coot: Model-building tools for molecular graphics. *Acta Crystallogr D Biol Crystallogr* 60:2126–2132.
26. Davis IW, et al. (2007) MolProbity: All-atom contacts and structure validation for proteins and nucleic acids. *Nucleic Acids Res* 35:W375–383.